Comparison of 3-D Deterministic Parallel and Monte Carlo Transport Computations for Special Nuclear Materials Assessments

Gabriel Ghita*, Glenn E. Sjoden, and James E. Baciak

Florida Institute for Nuclear Detection and Security (FINDS), Department of Nuclear and Radiological Engineering, University of Florida, Gainesville, FL, 32606, USA

Abstract

This paper discusses several topics related to our efforts to accomplish research leveraging 3-D radiation transport models to ultimately yield a complete mosaic of the radiation spectrum from a fissile source. Here, we effectively characterize and construct SNM neutron source terms, and demonstrate that the BUGLE-96 multigroup library is applicable to our general deterministic transport neutron detection scenarios.

We also investigated our initial design of a moderated He-3 detector array. In performing our computations, we demonstrate how the PENTRAN parallel 3-D Sn code is quite efficient at parallel computation with several domain decomposition strategies, achieving a parallel (Amdahl) fraction of 0.96 on up to 16 dedicated processors while yielding our adjoint Sn transport results. Finally, we have established a procedure for analyzing He-3 response in a graded detector-moderator array, and are moving closer in our efforts to attribute a neutron spectrum from the resulting neutron responses in our graded moderator He-3 detector array, simulated entirely via computational methods for SNM sources of high interest.

KEYWORDS: He-3, SNM Detection, PENTRAN, Parallel, Adjoint Sn

1. Introduction

The detection of Special Nuclear Materials (SNM) is of critical importance in the ongoing efforts to secure free nations. To yield an accurate profile of the neutron spectrum emanating from a fissile source, various configurations of moderating and attenuating materials can be placed around an array of He-3 tubes in order to isolate different parts of the neutron spectrum, although significant optimization studies are necessary; this is possible using numerical radiation transport simulations. For neutron detection with He-3 gas proportional counters, transport simulations must be applied to predict the optimum number of neutron interactions in He-3 to facilitate positive detection and characterization of the neutron source. Augmenting gamma spectrometry, research leveraging 3-D radiation transport models is being used to ultimately yield a complete mosaic of the radiation field from a fissile source [1]. This paper presents a summary of work performed under FINDS at the University of Florida to perform a comparative

* Tel. 352-870-0692, E-mail: ghita1gm@ufl.edu

analysis of deterministic parallel and Monte Carlo radiation transport results related to the generation, transport, and detection of leakage radiation sources. Sources are attributed to candidate masses of Special Nuclear Materials (SNM) for investigating computational nuclear materials detection scenarios. In this paper, we consider Pu metal and oxide SNM sources, with subsequent response through interactions in detectors predicted by computational transport methods. Overall, this work will culminate in an optimal design and demonstration of a neutron detector array, augmented with gamma detection, to serve as an SNM screening system for parcels. Radiation Transport models are being accomplished on high performance computers using PENTRAN (Parallel Environment Neutral Particle TRANsport) [2] via forward and adjoint Sn transport simulations with various multigroup libraries validated independently using Monte Carlo (MCNP5) [3] simulations. In Section 2, we discuss total source construction procedures for SNM modeling scenarios. In Section 3, we follow with a synopsis of Computational Pu SNM Sources, including both metal and oxide. In Section 4, we discuss parallel transport computations for our moderated He-3 array [4], followed by conclusions and future work, etc.

2. Total Source Construction for SNM Modeling

2.1 Assembly of Source Components

In assembling the source terms leaking from an SNM mass, the sources are composed of (i) intrinsic (spontaneous fission, (n,2n), etc) neutron (and gamma ray) sources, and (ii) induced fission neutron (and gamma) radiation as a result of multiplication within the assembly [1,5]. These sources can be categorized as follows:

Intrinsic (s.f. etc, reactions) neutron source density: $Q_{o,n}$ n/cm^3/s (1)

Induced (multiplied) neutron source density: $-\frac{Q_{o,n}}{\rho}$ n/cm^3/s (2)

where System *Reactivity* is based on fission multiplication: $\rho = \frac{k_{eff} - 1}{k_{eff}}$

Note that for this work, we consider only neutrons, and assume that any SNM material is completely uniform, so that the source density terms are constant for the SNM mass considered in a given configuration. Since reactivity ρ is based on a sub-critical configuration (and therefore must be < 0) determined from a criticality eigenvalue computation, the sum of the two sources constitutes the total SNM neutron source, accounting for both intrinsic neutrons and subcritical multiplication of those neutrons throughout the fissile material volume V, where:

Total n (multiplied) source: $M_n = \frac{Q_{o,n} V}{1 - k_{eff}}$ n/s (3)

The total detectable neutron source is rendered using the *probability of leakage* from the assembly, determined from a transport computation (since only the leaking radiation can be detected), resulting in the so-called 'leakage multiplication' source:

Total 'leakage multiplication' n source: $M_{L,n} = M_n \cdot P_{L,n} = \frac{Q_{o,n} V P_{L,n}}{1 - k_{eff}}$ n/s (4)

The detectable neutron and fission gammas generated, accounting for *leakage multiplication*, are determined from a sum of both intrinsic sources and subcritical multiplication in the assembly. For practical detection scenarios, multiple transport computational assessments are required as the potential for spectrally dependent reflection with varying geometry occurs. While it is useful to verify the comparable amounts of source radiation in an unreflected configuration, "SNM in free air" computational criticality assessments for both the plutonium and uranium cases accomplished via Monte Carlo or deterministic calculations must be updated with surrounding geometry issues that affect overall leakage and potential reflection, etc.

2.2 Leakage Source Spectral Dependence

While the total source as defined in Equations (1) through (4) is important, computational models must capture the spectral fidelity of radiation from SNM materials transporting through the geometry to assess the absolute, computationally determined detectable radiation from SNM material. For neutrons, the energy-dependent leakage (signified using an energy group subscript *g*) per induced fission reaction due to multiplication of the intrinsic source is computed via either deterministic or Monte Carlo radiation transport computations, and added to the leakage computed using the intrinsic (spontaneous fission, (n,2n), etc) source alone (also determined from transport computations):

$$M_{L,g_n} = \frac{\int_A \vec{J}\,|_{A\ \text{induced}-n,g} \cdot d\vec{A}}{\sum_{g=1}^{G} \int_V Q_{\text{induced}-n,g}\, dV} \cdot \left(-\frac{Q_{o,n} V}{\rho} \right)_{\text{induced}-n} + \int_A \vec{J}\,|_{A\ \text{intrinsic}-n,g} \cdot d\vec{A} \qquad (5)$$

where:

-- $\int_V Q_{\text{induced}-n,g}\, dV$ is the energy group *g induced* fission neutron source from a criticality computation, where *V* constitutes the volume of SNM mass in the system

-- $\int_A \vec{J}\,|_{A\ \text{induced}-n,g} \cdot d\vec{A}$ is the energy group *g induced* fission neutron leakage at the SNM material surface, where *A* constitutes the surface area of the SNM mass in the system

-- $\int_A \vec{J}\,|_{A\ \text{intrinsic}-n,g} \cdot d\vec{A}$ is the energy group *g intrinsic* neutron leakage at the SNM material surface, where *A* constitutes the surface area of the SNM mass in the system

-- $\left(-\frac{Q_{o,n} V}{\rho} \right)_{\text{induced}-n}$ is equal to Equation (2) multiplied by the SNM volume *V*.

Using Equation (5), the Total leakage multiplication source is determined from a sum of the total source from all energy groups:

$$M_{L,n} = \sum_{g=1}^{G} M_{L,g_n} \qquad (6)$$

Note that the total leakage multiplication source determined by Equation (6) is identical to the total leakage multiplication source determined using Equation (4). An important fact is that the source term of Equation (5) can be used to identify specific energies in the leakage spectrum which can be computationally optimized using filters (e.g. Al, Cd, In, etc) and various moderators with transport computations. We note that a similar set of equations describe the gamma rays (intrinsic and induced) leaking from the SNM system, although the focus of our work here is on neutron transport. For an SNM mass in a "free air" system, the net neutron or gamma currents (leaking) crossing the outer SNM surface are approximately equal to the exiting (positive outward normal) partial current, or $\vec{J}_g|_A = (\vec{J}_g^+|_A - \vec{J}_g^-|_A) \approx \vec{J}_g^+|_A$, since almost no neutrons (or gammas) exiting from an assembly placed in air return into the multiplying system (e.g. ~1 in 10^4 neutrons and ~0.5 in 10^4 gamma rays return for a 4 kg Pu (94% Pu-239) alpha-metal sphere). As mentioned earlier, other structures impacting the detection scenario will result in neutrons or gammas from higher energies streaming from the assembly to scatter in surrounding materials, lose energy, and subsequently appear in lower energies (higher energy *group* numbers), creating attributable re-entrant currents at the SNM surface ($\vec{J}_g^-|_A$). As mentioned, these must be evaluated on a case-by-case basis as a function of position (and time) since multiplication can be affected.

2.3 Cross Section Library and Code Considerations

Since computational transport methods are necessary to determine total leakage multiplication sources for specific source scenarios, adequate cross section libraries must be applied. Many Monte Carlo users can readily access point-wise cross sections in MCNP5, although care needs to be taken to select appropriate thermal treatments and library temperatures. Deterministic Sn cross section libraries must be evaluated carefully as to how they are applicable to a given problem. Reasonable agreement between Monte Carlo and deterministic results should be expected, and questions should be raised to explain differences. Based on available data for transport computations, to demonstrate consistency between deterministic and Monte Carlo transport computations, we have considered:

(i) The MCNP5 Monte Carlo code using continuous energy ENDF/B-VI data libraries 293.6K and
(ii) The PENTRAN Parallel Sn Code using BUGLE-96 [6] broad group library derived from ENDF/B-VI, 47 group neutron (and if required, coupled 20 group gamma)

MCNP5 is the well known LANL Product, and uses the latest point-wise ("continuous") energy data based on the latest ENDF/B-VI. We note that for proper thermal treatment, $S(\alpha,\beta)$ light element thermal neutron molecular scattering effects must be used.

PENTRAN is a 3-D anisotropic deterministic multigroup Sn code with a capability to automatically distribute itself on parallel cluster architecture by decomposing the problem among angular, energy group, and spatial variables, thus performing hybrid parallel decompositions. Under development over more than 10 years, PENTRAN has a number of advanced numerical features and has demonstrated highly scalable parallel performance.

3. Computational Pu SNM Sources

3.1 Summary of Plutonium SNM Intrinsic Source Determinations

The intrinsic radiation from plutonium is inherently dependent upon the content and irradiation history (burnup) that the fuel underwent in the reactor that produced it. To develop our source terms, burnups were computed with different reactor fuels for varying times using the SCALE5 [7] package to yield the ending isotopic content of plutonium discharged from a reactor following burnup, with chemical separation/purification into spherical 4 kg masses.

3.1.1 Pu Mass Material Assumptions

Burnup was simulated with the SCALE5 package for CANDU-37 reactor fuel (with 37 pins, natural UO_2) for the durations of 888, 2643, 4404 and 7928 Mega-Watt Days/Metric-Ton of heavy metal (MWD/MT), corresponding to power reactor irradiation times of 25.3, 75.5, 125.8, and 226.5 days. The weight percents of the different isotopes of plutonium metal (Pu-238, Pu-239, Pu-240, Pu-241, and Pu-242) were considered (note Pu-243 existed in very trace amounts, and was neglected). A density of the alpha-phase plutonium equal to 19.86 grams/cubic centimeter was used for our standard Pu metal source containing 1 ppm oxide, defined as a 4 kilogram spherical ball, and the mass of each isotope was calculated from the Pu isotopic concentrations. Similar procedures and calculations were carried out for plutonium oxide spheres, where an oxide density of 10.59 grams/cubic centimeter was used (a 92.5% of PuO_2 theoretical density of 11.46 grams/cubic centimeter). The Pu metal spheres had a radius of 3.636 cm, while the Pu oxide spheres had a radius of 4.484 cm.

3.1.2 Intrinsic and Induced Source Determinations

Isotopic information was defined in ORIGEN-ARP [7] to determine the intrinsic neutron and gamma energy spectrum both initially and after a 10 year Pu aging period. A 67-group BUGLE-96 energy bin structure was used in SCALE5 to assess the spectra information. The neutron multiplication eigenvalue (k_{eff}) to compute the induced neutron radiation component was determined using the MCNP5 Monte Carlo code. Several eigenvalue cases were also run using PENTRAN with BUGLE-96 library.

Table 1: Variation of k_{eff} determined from MCNP5 from Pu from CANDU fuel

	MCNP5 *k-eff*, CANDU fuel			
	Pu Metal		*PuO2*	
MWD/MT	k_{eff}	1-σ rel	k_{eff}	1-σ rel
888	0.75344	0.00064	0.49398	0.00049
2643	0.73733	0.00062	0.48232	0.00044
4404	0.72400	0.00061	0.47293	0.00044
7928	0.70196	0.00054	0.45801	0.00041

As a trend for the plutonium metal and oxide, the shorter the irradiation time, the higher the Pu-240 content, leading to higher relative source strengths with more intrinsic neutrons emitted due to spontaneous fission reactions. The spheres with plutonium derived from the longest

irradiation times have higher neutron and gamma emission rates, as expected. Details of the intrinsic source spectra are in Fig. 1.

Figure 1: 4 kg intrinsic neutron source spectra from (a.) Pu-α metal, and (b.) Pu-oxide as a function of neutron energy

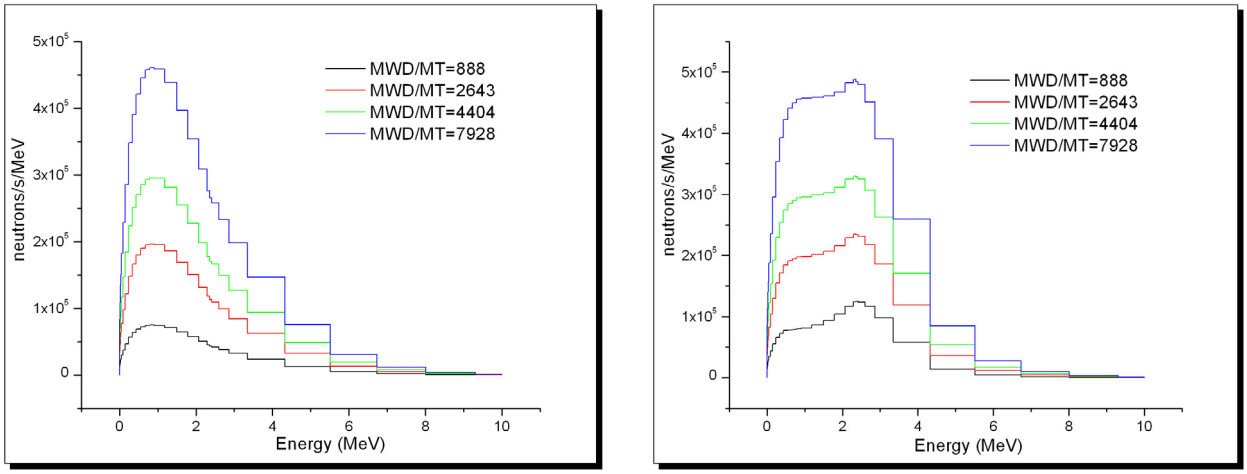

3.2 Intrinsic Source Trends

For plutonium metals, most of the intrinsic neutron source comes from spontaneous fission (s.f.) in even numbered isotopes, and Pu-240 can be attributed to over 90% of the s.f. reactions, with the remainder dominated by Pu-242, and Pu-238. Therefore, the intrinsic neutron source increases with burnup irradiation of the fuel that produced the plutonium; this trend is also true for the intrinsic gamma source spectrum. For plutonium oxides, the intrinsic neutron source term is often ~twice that of Pu metal (a rough rule of thumb--it can be more or less depending upon specific SNM parameters), since the presence of oxygen results in a significant light element (α,n) component, dominated by these reactions attributed to Pu-239, Pu-238, Pu-240, and Am-241 in aged samples. As with metal, the intrinsic neutron source increases with burnup irradiation of the fuel that produced the plutonium. This trend is also true for the intrinsic gamma source spectrum; the gamma spectrum is close to that of the metal, although it tends to be slightly softer.

3.3 Monte Carlo (MCNP5) and Sn (PENTRAN/BUGLE-96) intrinsic and induced n-leakage

The intrinsic source leakage from the 4 kg Pu metal ball was computed using Monte Carlo methods using the MCNP5 code with ENDF/B-VI cross sections, and using 3-D Sn methods using PENTRAN with the BUGLE-96 47 group neutron library. The flux solution projected onto an *x-y-z* mesh for fast neutrons for a 1/8 symmetry sphere using a deterministic computation is shown in Figure 2a. Values for the group leakage from the ball were compared between Monte Carlo (using continuous energy, equivalent group energy bin tallies) and deterministic Sn; values

compared well for the intrinsic source leakage. The continuous energy Monte Carlo group binned leakage versus Sn rendered multigroup leakage is given in Fig. 2b.

Figure 2: 4 kg Pu-metal ball in air, using intrinsic neutron source spectra from (a.) fast flux solution projected on Sn 1/8 symmetry mesh (b.) Plot of Monte Carlo (MCNP5--ENDF/B-VI) and Sn (PENTRAN--BUGLE-96) intrinsic Pu-metal leakage source over 47 energy groups

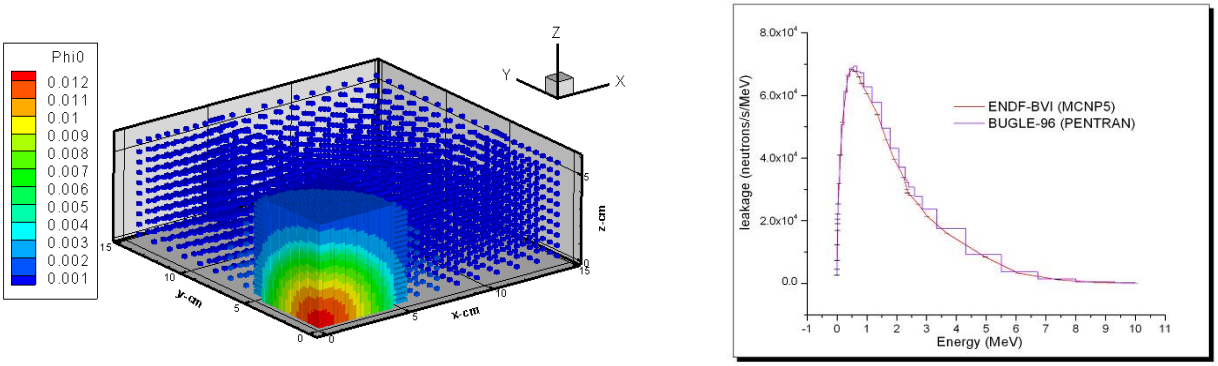

a. b.

Regarding computation of the induced radiation leakage source component (ref Equation (5)), we have found that MCNP5 Monte Carlo code criticality computations are more straightforward for k_{eff} determinations. While the BUGLE-96 library is reasonably adequate for shielding computations, we found that fast metal criticality computations were less accurate with BUGLE-96; neutron leakage was 2.6% lower than with the Monte Carlo computation, which caused k_{eff} to be ~10% higher with the BUGLE-96 library than Monte Carlo result. This can be accounted for, since the BUGLE-96 was produced as a coupled shielding library weighted using power reactor fluxes, which does not fit modeling induced multiplication in small SNM sources.

4. He-3 Moderator Array Assembly

4.1 Neutron Moderator Bank for He-3 n-Detection

In support of our SNM detection efforts for parcel screening, we are working to selectively thermalize specific parts of the neutron spectrum for eventual spectral unfolding using He-3 detectors with graded moderators. As fast neutrons thermalize via collisions in a moderator, the potential for subsequent neutron detection in a nearby He-3 detector (undergoing an (n,p) reaction, with $Q=0.764$ MeV) increases rapidly with thermalization. Toward this goal, a number of neutron moderators were selected and analyzed to evaluate them for (n,p) response in He-3. A He-3 based moderator bank geometry, shown in Fig. 3, was established to perform 3-D Sn forward and adjoint computations using the parallel PENTRAN code with responses (R) computed using Pu metal and oxide leakage surface source planes.

R can be determined using either a forward (integrating over all phase space reactions in He-3) or an adjoint (integrating over the phase space product of the actual source term and adjoint function relative to a He-3 tube bank adjoint source response) using the relation:

$$R = \left\langle \psi_g \sigma_{d\,g} \right\rangle = \left\langle \psi_g^{+} q_g \right\rangle \qquad (7)$$

Figure 3: Moderated He-3 Tube Bank

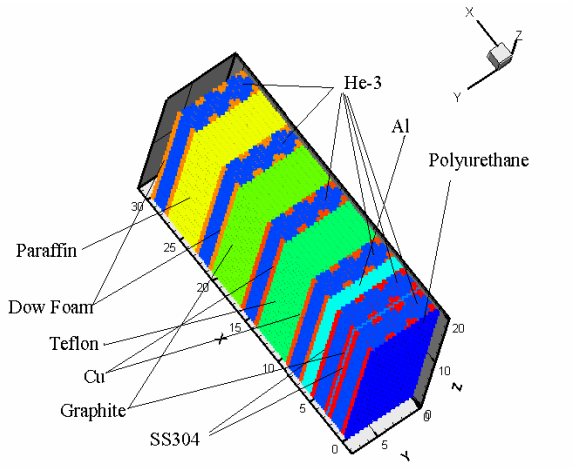

Therefore, detector response can be obtained by complete integration of the source distribution with the adjoint function for any arbitrary source distribution.

4.2 3-D Parallel Sn Computational Performance

Using an adjoint source in the 5th He-3 tube bank for the discretized model in Fig. 3 (using 36,900 3-D mesh cells with the BUGLE-96 multigroup library), several parallel S16 P3 computations of the neutron adjoint were computed using the PENTRAN Code on up to 16 dedicated processors composed of 64-bit processors with 4 Gb of RAM.each. The 16 processor run using angular decomposition required 1h 18 min to complete.

Table 2: Parallel PENTRAN Adjoint Results for He-3 Moderator Bank using various Decompositions of the Angular, Energy, and Spatial domains of the const. size problem

.

Run	PENTRAN Decomposition Strategy	# Procs Angle	# Procs Group	# Procs Space	# Total Procs (P)	Sp= Speed-up Factor	Ef= Efficiency (Sp/P, %)
1	Angular	4	1	1	4	3.85	96.25
2	Spatial	1	1	6	6	3.94	66
3	Angular	8	1	1	8	6.54	82
4	Angular-Spatial	4	1	3	12	7.73	64
5	Angular-Spatial	4	1	4	16	9.47	59
6	Angular	16	1	1	16	10.89	68

Figure 4: Parallel Speedup with Amdahl's Law Projection

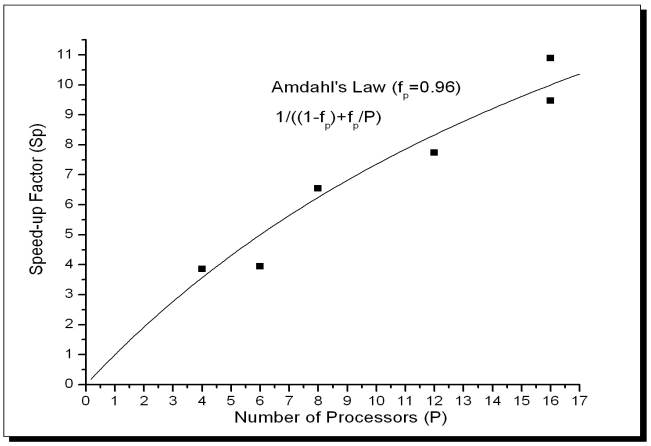

Plotting Table 2 speedup data in Figure 4, and using Amdahls' law to project a speedup curve with a constant parallel fraction *fp*, we found that the PENTRAN code yielded a parallel fraction of 0.96 for this problem. These results confirm that PENTRAN is highly scalable, maintaining consistent speedup performance results with various domain decomposition strategies.

4.3 Comparison of Forward, Adjoint, and Monte Carlo Results

We completed 3-D Transport models (Ref Fig. 3) using forward & adjoint Sn, and Monte Carlo (a schematic of the 3-D MCNP5 tube bank is shown in Fig. 5) using our design for a He-3 Moderator array for both Pu-Metal and Pu-oxide sources. As shown in Table 3, excellent agreement was achieved for computation of the reaction rate in He-3 tubes banks in cells 2, 4, 6, 8, 10 or 12, as indicated. Reaction rate results from the adjoint computations were higher due to the use of an equivalent isotropic source striking the polyurethane cell on the front panel of the assembly folded with a scalar adjoint in that cell, rather than coupling the response using angular data. For this reason, the adjoint results will always slightly over-predict the reaction rate. Future work will involve using angular data to couple the reaction rate.

Figure 5: MCNP5 Model of He-3 Bank

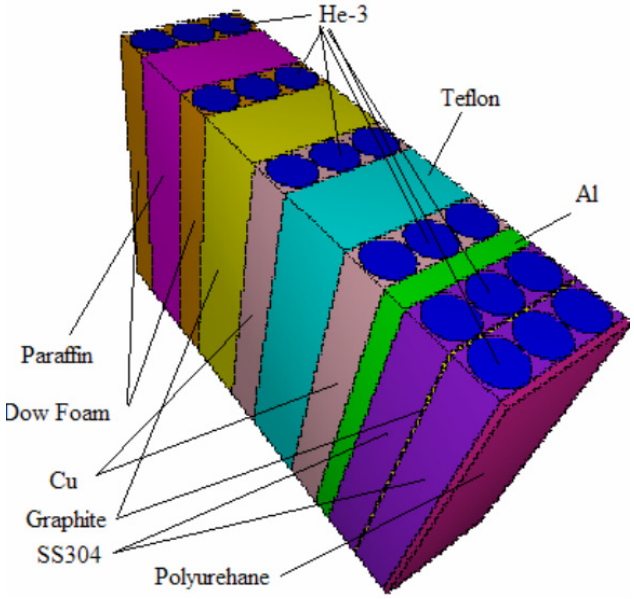

Table 3: Comparison of Reaction Rates in Each He-3 Tube bank using Forward Sn, Adjoint Sn, and Monte Carlo Results

a. Pu metal

Cel #	PENTRAN (BUGLE-96) -forward-	PENTRAN (BUGLE-96) -adjoint-	MCNP5 (ENDF-BVI) -forward-	Rel. error (MCNP5)	Rel. diff. (%) PEN(fwd)vs MCNP
2	17.36	18.228	15.82399	2.27503E-4	9.71
4	6.961	7.95609	6.67756	6.22982E-4	4.25
6	3.285	4.4268	3.13771	0.00248	4.69
8	1.726	3.44596	1.71623	0.01573	0.57
10	13.79	13.72829	13.19437	0.0088	4.51
12	10.93	10.78577	10.7144	0.00943	2.01

b. Pu oxide

Cel #	PENTRAN (BUGLE-96) -forward-	PENTRAN (BUGLE-96) -adjoint-	MCNP5 (ENDF-BVI) -forward-	Rel. error (MCNP5)	Rel. diff. (%) PEN(fwd)vs MCNP
2	12.74224	13.37935	11.6209	6.9282E-4	9.65
4	5.09863	5.82949	4.8915	0.00162	4.24
6	2.39915	3.23938	2.28576	0.00676	4.96
8	1.26867	2.53109	1.31515	0.04894	3.53
10	10.13477	10.06012	9.953	0.02657	1.83
12	8.06372	7.95435	7.8356	0.02904	2.91

Referring to the results in Table 3, the relative difference among the values is highest for the He-3 tube bank closest to the front polyurethane panel, since the Monte Carlo stochastic error is higher for this bank (due to a low relative fraction of thermal neutrons from the Pu sources), and due to the use of an average scalar adjoint coupling, which is more sensitive to short transport distances. Overall, very good agreement was obtained given that the Monte Carlo implemented continuous energy ENDF/B-VI cross sections, and the Sn computations were accomplished via the multigroup BUGLE-96 library.

5. Conclusions and Future Work

Overall, results in this paper demonstrate that we effectively constructed the neutron source terms, and that the BUGLE-96 library is applicable to shielding and moderation transport problems contributing to the design of a moderated He-3 detector array. In addition, we showed how the PENTRAN code is quite efficient at 3-D parallel computation with various decomposition strategies, achieving a parallel (Amdahl) fraction of 0.96 scaling up to 16 dedicated processors. Finally, we have established a procedure for analyzing He-3 response in a graded He-3 detector-moderator array, and are moving closer in our efforts to extract a neutron spectrum from the resulting responses, simulated entirely computationally for two SNM sources of interest.

Acknowledgement

This work was supported by the National Nuclear Security Administration.

References

1) Reilly, et al, Passive Nondestructive Assay of Nuclear Materials, USNRC/Los Alamos National Laboratory, NUREG/CR-5550, (1991).
2) Sjoden, G., and A. Haghighat, "PENTRAN - A 3-D Cartesian Parallel Sn Code with Angular, Energy, and Spatial Decomposition," Proc. of the Joint Int'l Conf on Mathematical Methods and Supercomputing for Nuclear Applications, Vol I, p. 553, Saratoga Springs, New York (1997).
3) X-5 Monte Carlo Team, "MCNP-A General Monte Carlo N-Particle Transport Code, Version 5 Volume II: User's Guide," Los Alamos National Laboratory, Report LA-CP-03-0245, (2003).
4) Ghita, G., G. Sjoden, and J. Baciak, "3D Computational and Experimental Radiation Transport Assessments of PuBe Sources and Graded Moderators for Parcel Screening", Proc. Defence & Security Symposium, Orlando, FL, USA, April 17-21, 2006, to be published.
5) Duderstadt, J. and L. Hamilton, Nuclear Reactor Analysis, Wiley, (1976).
6) White, J., et al., "BUGLE-96: A Revised Multi-group Cross Section Library for LWR Applications Based on ENDF/B-VI Release 3", DLC-185, Oak Ridge National Laboratory, Oak Ridge, TN (1996).
7) "SCALE: A Modular Code System for Performing Standardized Computer Analyses for Licensing Evaluations," ORNL/TM-2005/39, Version 5, Vols. I–III, (April 2005).